

The pilus usher controls protein interactions via domain masking and is functional as an oligomer

**Glenn T. Werneburg^{1,2}, Nadine S. Henderson^{1,2},
Erica B. Portnoy^{1,2}, Samema Sarowar^{3,4}, Scott J. Hultgren^{5,6},
Huilin Li^{3,4}, and David G. Thanassi^{1,2}**

¹ Center for Infectious Diseases, Stony Brook University,
Stony Brook, New York, USA

² Department of Molecular Genetics and Microbiology, Stony Brook University,
Stony Brook, New York, USA

³ Department of Biochemistry and Cell Biology, Stony Brook University,
Stony Brook, New York, USA

⁴ Biosciences Department, Brookhaven National Laboratory,
Upton, New York, USA

⁵ Department of Molecular Microbiology, Washington University
School of Medicine, Saint Louis, Missouri, USA

⁶ Center for Women's Infectious Disease Research, Washington University
School of Medicine, Saint Louis, Missouri, USA

Submitted to Nature Structural & Molecular Biology

November 2014

**Biological, Environmental & Climate Sciences Department
Brookhaven National Laboratory**

Prepared for U.S. Department of Energy

Notice: This manuscript has been authored by employees of Brookhaven Science Associates, LLC under Contract No. DE-SC0012704 with the U.S. Department of Energy. The publisher by accepting the manuscript for publication acknowledges that the United States Government retains a non-exclusive, paid-up, irrevocable, world-wide license to publish or reproduce the published form of this manuscript, or allow others to do so, for United States Government purposes.

DISCLAIMER

This report was prepared as an account of work sponsored by an agency of the United States Government. Neither the United States Government nor any agency thereof, nor any of their employees, nor any of their contractors, subcontractors, or their employees, makes any warranty, express or implied, or assumes any legal liability or responsibility for the accuracy, completeness, or any third party's use or the results of such use of any information, apparatus, product, or process disclosed, or represents that its use would not infringe privately owned rights. Reference herein to any specific commercial product, process, or service by trade name, trademark, manufacturer, or otherwise, does not necessarily constitute or imply its endorsement, recommendation, or favoring by the United States Government or any agency thereof or its contractors or subcontractors. The views and opinions of authors expressed herein do not necessarily state or reflect those of the United States Government or any agency thereof.

The Usher Uses Domain Masking to Control Protein-Protein Interactions During Pilus Biogenesis and is Functional as an Oligomer *In Vivo*

Glenn T Werneburg^{1,2}, Nadine S. Henderson^{1,2}, Erica B. Portnoy^{1,2}, Samema Sarowar^{3,4}, Scott J. Hultgren^{5,6}, Huilin Li^{3,4}, and David G. Thanassi^{1,2,*}

¹Center for Infectious Diseases, Stony Brook University, Stony Brook, NY 11794-5120, USA

²Department of Molecular Genetics and Microbiology, Stony Brook University, Stony Brook, NY 11794-5222, USA

³Department of Biochemistry and Cell Biology, Stony Brook University, Stony Brook, NY 11794-5215, USA

⁴Biosciences Department, Brookhaven National Laboratory, Upton, NY 11973-5000, USA

⁵Department of Molecular Microbiology, Washington University School of Medicine, Saint Louis, MO 63110, USA

⁶Center for Women's Infectious Disease Research, Washington University School of Medicine, Saint Louis, MO 63110, USA

*Corresponding Author: David G. Thanassi, 242 Centers for Molecular Medicine Building, Stony Brook University, Stony Brook, NY 11794-5120, USA. Phone: 631-632-4549; Fax: 631-632-4294; Email: david.thanassi@stonybrook.edu

ABSTRACT

The chaperone/usher (CU) pathway is responsible for biogenesis of organelles termed pili or fimbriae in Gram-negative bacteria. Type 1 pili expressed by uropathogenic *Escherichia coli* are prototypical structures assembled by the CU pathway. Assembly and secretion of pili by the CU pathway requires a dedicated periplasmic chaperone and a multidomain outer membrane protein termed the usher (FimD). We show that the FimD C-terminal domains provide the high-affinity substrate binding site, but that these domains are masked in the resting usher. Domain masking requires the FimD plug domain, which serves as a central switch controlling usher activation. We demonstrate that usher molecules can act *in trans* for pilus biogenesis, providing conclusive evidence for a functional usher oligomer. These results reveal mechanisms by which molecular machines such as the usher regulate and harness protein-protein interactions, and suggest that ushers may interact in a cooperative manner during pilus assembly in bacteria.

INTRODUCTION

The chaperone/usher (CU) pathway is a conserved secretion system that is widely distributed among Gram-negative bacteria¹⁻³. The CU pathway is dedicated to the assembly of virulence-associated organelles termed pili or fimbriae. Pili are hairlike fibers that extend out from the bacterial surface and mediate diverse cellular functions, including adhesion to host cells and biofilm production⁴. The type 1 and P pili expressed by uropathogenic *Escherichia coli* (UPEC) are prototypical structures used as model systems for the CU pathway. Type 1 and P pili are critical virulence factors of UPEC, allowing colonization of the bladder and kidney, respectively^{5,6}.

CU pili are linear polymers composed of multiple different subunit proteins (pilins). The assembled pilus adopts a composite architecture on the bacterial surface, consisting of a rigid helical rod that is anchored to the outer membrane (OM) and a distal, flexible tip fiber that contains the adhesive subunit (adhesin). The type 1 pilus rod contains more than 1,000 copies of the FimA major pilin; the type 1 pilus tip contains the FimH adhesin at its distal end, followed by single copies of the FimG and FimF adaptor subunits (Fig. 1a)^{7,8}. The FimH adhesin binds to mannosylated proteins present on the bladder epithelium, leading to bacterial invasion, the establishment of infection, and the development of cystitis⁵. The CU pathway assembles and secretes pili in a highly regulated manner (Fig. 1a). Nascent pilins enter the periplasm via the Sec translocon⁹, and then form binary complexes with the periplasmic chaperone in a process termed donor-strand complementation (DSC)^{10,11}. In DSC, the chaperone donates one of its β -strands to complete the incomplete immunoglobulin (Ig)-like fold of the subunit, thus allowing folding of pilus subunits into stable structures (Supplementary Fig. 1a)¹⁰⁻¹². For assembly of subunits into a pilus fiber and secretion of the fiber to the cell surface, chaperone-subunit complexes must interact with the OM usher. The usher catalyzes the exchange of chaperone-

subunit for subunit-subunit interactions¹³. Subunit-subunit interactions form by a mechanism termed donor strand exchange (DSE), in which the N-terminal extension (Nte) of an incoming subunit displaces the donated chaperone β -strand from the preceding subunit, thereby completing the Ig fold of the preceding subunit (Supplementary Fig. 1b)^{12,14}. Type 1 pili are assembled starting with the FimH adhesin, and the pilus extends by step-wise addition of new chaperone-subunit complexes to the base of the fiber (Fig. 1a). Each subunit specifically interacts with its appropriate neighbor in the pilus fiber, with the specificity of binding determined by the DSE reaction^{15,16}. In addition, the usher aids ordered pilus assembly by differentially recognizing chaperone-subunit complexes, with the usher having highest affinity for the initiating chaperone-adhesin complex¹⁶⁻¹⁹.

Ushers are large, integral OM proteins composed of five distinct domains: a periplasmic N-terminal (N) domain, a transmembrane β -barrel channel domain, a plug domain located within the β -barrel region that forms a channel gate, and two periplasmic C-terminal domains (C1 and C2) (Fig. 1 and Supplementary Fig. 1)²⁰⁻²³. The N domain provides the initial binding site for chaperone-subunit complexes and functions in the recruitment of complexes to the usher (Figs. 1a and 2a)^{21,24-26}. The C1 and C2 domains provide a second binding site for chaperone-subunit complexes and anchor the growing pilus fiber (Fig. 1a and Supplementary Fig. 2b)^{23,27,28}. In the resting *apo*-FimD usher, the plug domain occludes the lumen of the β -barrel channel (Supplementary Fig. 1c)^{20,22,23}. The usher must be activated for pilus biogenesis by binding of a FimC-FimH chaperone-adhesin complex to the N domain^{13,18,29}. Activation results in displacement of the plug to the periplasm, insertion of the FimH adhesin domain into the channel lumen, and transfer of FimC-FimH from the usher N domain to the C domains (Fig. 2b)²³. The mechanism and specific sequence of events driving activation and the handoff of chaperone-subunit complexes from the N to the C domains is not understood. The usher N and C domains bind to the same surface of the chaperone, and handoff requires rotation of the

chaperone-subunit complex, concomitant with translocation of the pilus fiber through the usher channel toward the cell surface^{21,23,26,27}. The usher exists in the OM as an oligomer^{20,28,30,31}. However, the pilus fiber is secreted through only one protomer of the usher oligomer, and the usher monomer appears to be sufficient for pilus biogenesis^{20,23,27,32}. Therefore, whether and how the additional usher molecules contribute to the catalysis of pilus assembly *in vivo* is a subject of debate.

In this study, we use site-directed photocrosslinking to confirm the usher N, C1, and C2 domains as specific binding sites for chaperone-subunit complexes during pilus assembly *in vivo*. Using a fluorescence-based affinity assay to compare binding of FimC-FimH to wild-type (WT) and domain deleted FimD ushers (Fig. 1b), we show that the FimD C domains provide the high-affinity binding site, suggesting that handoff of chaperone-subunit complexes from the N to the C domains is driven by differential affinity. We provide evidence that the C domains are masked in *apo*-FimD through interaction with the plug domain, explaining why FimC-FimH must first bind to the N domain to activate the usher. We show that the plug domain does not contribute to affinity for FimC-FimH, and is not required for initiating assembly of a pilus fiber. However, the plug is essential for fiber polymerization. Finally, by using a plug deletion mutant to pre-activate the usher, we demonstrate that co-expression of individually non-functional FimD mutants allows reconstitution of a functional pilus assembly platform, revealing that the usher is operational as an oligomer *in vivo*.

RESULTS

***In vivo* validation of the FimD N and C domains as binding sites for FimC-FimH**

chaperone-adhesin complexes. We used site-directed photocrosslinking via unnatural amino acid mutagenesis to map points of contact between FimC-FimH and the FimD usher, as predicted by two crystal structures: the isolated FimD N domain bound to a FimC-FimH pilin domain complex; and the complete FimD-FimC-FimH complex (Fig. 2a and b)^{21,23}. *Amber* stop codon (TAG) substitutions were constructed for residues in the N, C1 and C2 domains of FimD. Each FimD *amber* mutant was transformed together with a FimC-FimH expression plasmid into an *E. coli* strain containing plasmid pEVOL-pBpF. The pEVOL-pBpF plasmid encodes an *amber* suppressor tRNA and aminoacyl-tRNA synthetase, allowing incorporation of the photoreactive phenylalanine derivative *p*-benzoyl-phenylalanine (*p*Bpa) at the position of the *amber* stop codon³³. Following growth and induction for protein expression in the presence of *p*Bpa, the bacteria were exposed to UV light to promote reaction of the carbonyl oxygen of *p*Bpa with nearby carbon-hydrogen bonds, forming stable crosslinks^{33,34}. To identify crosslinked products, we purified the His-tagged ushers from bacterial lysates or examined OM fractions.

We constructed and analyzed nine different FimD *amber* mutants, obtaining crosslinks between the usher and the FimC chaperone or FimH adhesin for each mutant except one (Supplementary Fig. 3a). Each of these FimD *amber* mutants formed a stable usher in the OM in the presence of *p*Bpa, and each was functional for pilus assembly (data not shown). We obtained the strongest crosslinks when *p*Bpa was located at FimD positions F4, Y704, T717, or Y788 (Fig. 2 and Supplementary Fig. 3a). FimD F4 resides in the usher N domain and is predicted to contact FimC (Fig. 2a and Supplementary Fig. 2a)²¹. FimD Y704 and T717 are located in the C1 domain, and are predicted to contact FimH and FimC, respectively (Fig. 2b and Supplementary Fig. 2b)²³. FimD Y788 resides in the C2 domain and is predicted to contact

FimC (Fig. 2b and Supplementary Fig. 2b)²³. Crosslinked products that reacted with anti-FimC-FimH antibody were visible for each of these FimD *amber* mutants (Fig. 2c, top and middle panels). The anti-FimC-FimH antibody cross-reacts with the His-tag epitope, and thus also detects the His-tagged FimD usher. Immunoblotting with anti-His-tag antibody verified the presence of the usher in the crosslinked products, and analysis of a strain expressing a Strep-tagged FimD (which does not cross-react with the anti-FimC-FimH antibody) confirmed the presence of the chaperone or adhesin (Supplementary Fig. 3b and c). In addition, the crosslinked bands for the FimD F4, T717, and Y788 *amber* mutants, but not the Y704 mutant, reacted with anti-FimC-FimG antibody, which recognizes the FimC chaperone but not the FimH adhesin (Fig. 2d, bottom panel). Taken together, these results confirm the predicted interactions of FimD residues F4, T717, and Y788 with FimC, and FimD residue Y704 with FimH. More broadly, these results validate the N, C1, and C2 domains of the usher as specific binding sites for chaperone-subunit complexes during pilus biogenesis *in vivo*.

The bands obtained for the FimD F4 and Y788 *amber* mutants migrated at the expected size for a crosslinked FimD-FimC product (114 kDa; mature FimD and FimC are 91 and 23 kDa, respectively) (Fig. 2c). A doublet was obtained for the FimD F4 mutant, with the lower band migrating at the same position as the FimD-FimC complex obtained for the Y788 mutant. This lower band, but not the upper band, reacted with both the anti-FimC-FimH and anti-FimC-FimG antibodies, consistent with its identity as the usher-chaperone complex (Fig. 2c). Mass spectrometry analysis confirmed the presence of FimD and FimC in the lower FimD F4 band, as well as in the FimD Y788 crosslinked band (Supplementary Data Set 1). Mass spectrometry analysis of the upper band of the FimD F4 doublet suggested that this was a crosslinked product with the abundant OM protein OmpA (35 kDa) (Supplementary Data Set 1). This is consistent with the usher having a dynamic and flexible N domain, able to sample the periplasm for chaperone-subunit complexes. An *ompA* mutant strain assembled type 1 pili similarly to the

parental OmpA⁺ strain, as determined by hemagglutination (HA) assay (data not shown), indicating that that OmpA does not have a direct role in pilus biogenesis. In contrast to the FimD F4 and Y788 crosslinked products, the bands obtained for the FimD Y704 and T717 mutants migrated with slower relative mobility than expected for either a FimD-FimH complex (120 kDa; mature FimH is 29 kDa) or a FimD-FimC complex, respectively (Fig. 2c). Mass spectrometry confirmed the presence of FimH and FimC in the crosslinked bands, and did not identify other crosslinked partners for the FimD Y704 and T717 mutants (Supplementary Data Set 1). Therefore, we propose that these slower migrating bands represent FimD-FimD-FimH or FimD-FimD-FimC complexes, capturing the actively engaged usher oligomer during pilus assembly *in vivo*.

The FimD C1 and C2 domains provide the high-affinity binding site for FimC-FimH chaperone-adhesin complexes. Having validated the usher N and C domains as binding sites for chaperone-subunit complexes, we next sought to determine the relative contributions of each domain to affinity for FimC-FimH. Affinity was measured using an *in vitro*, fluorescence-based assay^{17,35}. Briefly, purified FimC-FimH complexes were labeled with the thiol-reactive probe coumarin maleimide (CPM) at a single introduced cysteine site in the FimC chaperone. CPM is sensitive to the polarity of its environment and increases in fluorescence as it is transferred from an aqueous to a protein environment. The association of purified FimD usher with CPM-labeled FimC-FimH was determined by quantitating the increase in fluorescence as FimD was incrementally added, allowing calculation of the apparent equilibrium bimolecular dissociation constant (K_d).

We first measured binding affinity of WT FimD for FimC-FimH, where FimC was labeled with CPM at Q19C, T51C, or N86C single cysteine substitution mutations. These labeling sites were chosen because of their close proximity to the usher when the chaperone-adhesin complex is

bound at either the N or C domains (Fig. 3 and Supplementary Fig. 4)^{21,23}. Each of the FimC substitution mutants expressed stably and functioned similarly to WT FimC for pilus assembly in bacteria (data not shown). Fluorescence binding assays using these FimC constructs yielded K_d of 9.50–12.6 nM (Fig. 3c and Supplementary Fig. 5). The measured affinities were not significantly different ($P = 0.18$), indicating agreement among the different labeling sites. Moreover, these values correspond well with a previously reported K_d of 9.1 nM, determined by surface plasmon resonance¹⁸. We chose the FimC_{Q19C} CPM labeling site ($K_d = 12.6$ nM) for subsequent affinity measurements.

To examine the contribution of the usher C domains to affinity for chaperone-subunit complexes, we measured the binding of FimD_{ΔC2} and FimD_{ΔC1ΔC2} domain deletion mutants to FimC-FimH. Both of these, and all other usher deletion mutants used in this study, expressed stably and folded properly in the bacterial OM (data not shown). We obtained a K_d of 213 nM for the FimD_{ΔC2} mutant, a 17-fold decrease compared to WT FimD (Fig. 3d and Supplementary Fig. 6a). Additional deletion of the C2 domain (FimD_{ΔC1ΔC2}) further decreased affinity of the usher for FimC-FimH to 389 nM (Fig. 3d and Supplementary Fig. 6b), a 31-fold decrease compared to WT FimD. The decreased affinities obtained for the FimD_{ΔC2} and FimD_{ΔC1ΔC2} mutants identify the C domains as the high-affinity binding site on the usher for chaperone-subunit complexes, and establish that both the C1 and C2 domains contribute to binding. These results also reveal that the usher N domain, which remains available for binding in the FimD_{ΔC2} and FimD_{ΔC1ΔC2} deletion mutants (Fig. 1b), has lower affinity for FimC-FimH compared to the C domains.

In the P pilus system, the isolated usher plug domain was shown to interact with chaperone-subunit complexes^{19,36}. To determine if the plug contributes to affinity for chaperone-adhesin complexes in the context of the full-length usher, we examined a FimD_{Δplug} mutant. The affinity

of FimD_{Δplug} for FimC-FimH (12.5 nM; Fig. 3d and Supplementary Fig. 6c) was similar to WT FimD. This indicates no direct role for the plug domain, at least for binding to the initiating chaperone-adhesin complex.

The plug domain masks the C domains in the inactive usher. Given that the C domains provide the high-affinity binding site, it is not clear why the N domain is required for the initial binding of chaperone-subunit complexes to the usher. To address this question, we measured the affinity of a FimD_{ΔN} mutant for FimC-FimH. Despite the presence of the C domains, there was no appreciable binding of FimC-FimH to FimD_{ΔN} ($K_d > 1200$ nM; Fig. 3d and Supplementary Fig. 6d). This suggests that the high-affinity C domains are unavailable for binding in the absence of the N domain. In its *apo* state, the usher plug domain resides within the lumen of the β -barrel channel (Supplementary Fig. 1c)^{20,22,23}. We reasoned that in this position, the plug could interact with the C1 and C2 domains, keeping the C domains inaccessible until activation of the usher by binding of a chaperone-adhesin complex to the N domain and expulsion of the plug to the periplasm. To test this, we constructed a FimD usher deleted for both the N and plug domains (FimD_{ΔNΔplug}) (Fig. 1b). The affinity of FimD_{ΔNΔplug} for FimC-FimH was 40.8 nM (Fig. 3d and Supplementary Fig. 6e), which is dramatically increased compared to the FimD_{ΔN} mutant and close to the affinity observed for WT FimD. This result indicates that the high-affinity C1 and C2 domains become accessible to chaperone-subunit complexes in the absence of the plug domain, supporting our hypothesis that the plug functions to mask the C domains in the inactive usher.

The plug domain is required for higher-order pilus assembly. Previous studies demonstrated that the plug domain is essential for pilus assembly by the usher^{22,37,38}. Our results here indicate that the plug domain functions to maintain the usher in the inactive state by masking the C domains, but this does not explain why the plug is necessary for pilus

biogenesis. One possibility is that, in the absence of the plug domain, chaperone-subunit complexes no longer bind to the N domain. We used site-directed photocrosslinking to detect binding of FimC-FimH to the FimD $_{\Delta\text{plug}}$ mutant. As shown in Figure 4, we obtained a similar pattern of crosslinks for the FimD $_{\Delta\text{plug}}$ mutant as for WT FimD when pBpa was located at usher positions F4 (N domain), T704 (C1), T717 (C1), or Y788 (C2). Thus, chaperone-subunit complexes still interact with both the N and C domains in the absence of the plug domain.

To further investigate the role of the plug in pilus assembly, we expressed His-tagged WT FimD or the FimD $_{\Delta\text{plug}}$ mutant in bacteria together with the FimC chaperone and the FimH and FimG pilus tip subunits. These experimental conditions allow testing of the ability of the usher to polymerize pilus fibers (consisting of FimH followed by multiple copies of FimG), using a co-purification assay³⁹. Pilus assembly intermediates that co-purified with the ushers from OM fractions were incubated in SDS sample buffer at either 25°C or 95°C, and then analyzed by immunoblotting with anti-FimC-FimG or anti-FimC-FimH antibodies. Subunit-subunit, but not chaperone-subunit, interactions are stable to SDS at low temperatures, so subunits that are assembled into a pilus fiber will shift to higher molecular mass when incubated at 25°C³⁹. Analysis of samples incubated at 95°C revealed that FimC, FimG, and FimH co-purified with both WT FimD and the FimD $_{\Delta\text{plug}}$ mutant (Fig. 5). Analysis of the WT FimD samples incubated at 25°C revealed a ladder of higher molecular mass species, indicating polymerization of FimG into a pilus fiber with FimH at its tip. In contrast, examination of the FimD $_{\Delta\text{plug}}$ samples incubated at 25°C demonstrated that the mutant was greatly impaired in its ability to promote fiber polymerization, with only bands corresponding to FimG-FimH and FimG-FimG-FimH assembly intermediates visible (Fig. 5). Consistent with this, bacteria expressing the FimD $_{\Delta\text{plug}}$ mutant were unable to assemble either FimG-FimH tip fibers or complete type 1 pilus fibers of sufficient length on the bacterial surface to agglutinate red blood cells (Supplementary Table 1). This is in contrast to bacteria expressing WT FimD, which exhibited robust HA activity. Taking these

findings together, we conclude that the plug domain is dispensable for the binding of chaperone-subunit complexes to the usher and initiation of pilus assembly, but essential for efficient polymerization of the pilus fiber.

Plug deletion reveals a functional usher oligomer. The usher exists as an oligomeric complex in the OM; however, only one usher protomer is involved in secretion of the pilus fiber, and the function of the usher oligomer is not known^{20,23,30-32}. One possibility is that the N domains of the non-translocating ushers recruit chaperone-subunit complexes to the OM assembly platform, thereby increasing the local concentration of chaperone-subunit complexes, and these complexes are then transferred to the C domains of the actively translocating usher. If true, then co-expression of FimD $_{\Delta C1\Delta C2}$ and FimD $_{\Delta N\Delta plug}$ usher mutants (N and C domains available, respectively; Fig. 6d) should allow reconstitution of pilus biogenesis. Indeed, co-expression of the $\Delta N\Delta plug$ and $\Delta C1\Delta C2$ FimD constructs resulted in assembly of functional type 1 pili, as measured by the HA assay (Table 1). Note that the $\Delta N\Delta plug$ and $\Delta C1\Delta C2$ mutants were not able to assemble pili when expressed individually (Table 1). Pilus biogenesis on the bacterial surface by the strain co-expressing the $\Delta N\Delta plug$ and $\Delta C1\Delta C2$ mutants was confirmed by electron microscopy (EM), which revealed levels of pilus fibers comparable to the strain expressing WT FimD (Fig. 6). Consistent with our finding that the C domains are masked by the plug domain in the inactive usher, co-expression of a FimD $_{\Delta N}$ mutant (plug domain intact) with FimD $_{\Delta C1\Delta C2}$ did not allow pilus assembly on the bacterial surface (Table 1). Thus, in this case, the C domains in the FimD $_{\Delta N}$ usher remain masked and unavailable for handoff from the N domain of the FimD $_{\Delta C1\Delta C2}$ usher. In additional experiments, we found that co-expression of FimD $_{\Delta N\Delta plug}$ with a FimD $_{\Delta plug\Delta C1\Delta C2}$ mutant did not restore pilus assembly, and neither did co-expression of FimD $_{\Delta N}$ with a FimD $_{\Delta plug\Delta C1\Delta C2}$ mutant (Table 1). This indicates that a plug domain must be present for successful complementation, but the plug cannot be located together with the C domains. These data demonstrate that individual usher molecules are capable of

functioning *in trans* for pilus biogenesis in bacteria. In addition, these data provide *in vivo* confirmation that the plug domain masks the C domains in the inactive usher.

DISCUSSION

The usher is a remarkable molecular machine that catalyzes ordered polymerization of the pilus fiber and provides the channel for secretion of the fiber to the cell surface. The usher performs its functions in the absence of an external energy source such as ATP, relying instead on harnessing protein-protein interactions⁴⁰. The usher contains five distinct domains, each of which is essential for pilus biogenesis. Our findings reveal mechanisms by which the usher controls access to its domains and show how these domains act in concert to ensure the assembly of adhesive organelles. We also demonstrate that individual usher molecules can act *in trans* for pilus biogenesis in bacteria, providing conclusive evidence for a functional usher oligomer.

Using site-directed photocrosslinking in intact bacteria, we confirmed that the usher N, C1, and C2 domains function as binding sites for chaperone-subunit complexes during pilus biogenesis *in vivo*. Our crosslinking studies also captured higher-order FimD-FimC-FimH pilus assembly intermediates. Other binding partners were not identified by mass spectrometry analysis of the crosslinked products, and only the usher is capable of forming a crosslink in our experimental system. Therefore, we propose that these higher-order assembly intermediates comprise FimD-FimD as well as FimD-FimC-FimH contacts, consistent with the usher oligomer forming an actively engaged assembly unit *in vivo*. However, we do not yet know the exact nature of the crosslinked products or the basis for the altered mobilities of the FimD Y704 and T717 crosslinked bands. The *pBpa* crosslinking residue for these higher-order complexes was located in the FimD C1 domain (at Y704 or T717), implicating the C1 domain as a site of usher-usher contact. This is consistent with previous results showing that deletion of the C domains altered the dimerization interface of the P pilus usher PapC³¹.

Our comparison of full-length and domain-deleted FimD ushers revealed that the C1 and C2 domains provide the high-affinity binding site for FimC-FimH chaperone-adhesin complexes. We found that the plug domain is not required for the usher to form high-affinity interactions with FimC-FimH. Therefore, we conclude that the K_d measured for WT FimD (12.6 nM) reflects the contribution of the C domains to affinity for FimC-FimH, and the K_d measured for FimD $_{\Delta C1\Delta C2}$ (389 nM) reflects the contribution of the N domain to affinity for FimC-FimH. Previous studies of the isolated FimD N domain measured a K_d of ~900 nM for binding to FimC-FimH,^{16,41}. This value is within ~2-fold of our value measured for FimD $_{\Delta C1\Delta C2}$, supporting our interpretation that this mutant reports affinity of the N domain. In contrast to our results, Volkan *et al.* found that the C2 domain of the P pilus usher PapC had lower affinity for chaperone-subunit complexes compared to the N domain¹⁹. This difference likely reflects the fact that the PapC C2 domain was studied in isolation, rather than in its native orientation in the context of the rest of the usher protein. In particular, the C1 domain may be critical for proper interaction with chaperone-subunit complexes. Indeed, we previously demonstrated that mutation of a residue in the PapC C1 domain (R652A) resulted in a loss of high-affinity binding of PapD-PapG to the full-length usher¹⁷. Chaperone-subunit complexes bind first to the usher N domain and then transfer to the C domains, through an unknown mechanism^{21,23-25,27,28}. Our results suggest that this handoff is driven by differential affinity, with the high affinity C domains successfully competing with the lower affinity N domain for the common binding site on the chaperone. Handoff may also be facilitated by allosteric destabilization of the N domain-chaperone-subunit complex by the C2 domain or through interactions with the plug, as suggested by recent studies in the P pilus system^{19,36}.

Our finding that the C domains have higher affinity compared to the N domain for FimC-FimH raised the question as to why chaperone-subunit complexes first bind to the N domain of the *apo* usher. By comparison of ΔN and $\Delta N\Delta\text{plug}$ FimD deletion mutants, we demonstrated that

the C domains are not available for binding in the absence of the N domain, but become available in the absence of the plug. Based on these results, we propose that the *apo* usher employs a domain masking strategy to keep the C domains inaccessible, dependent on interaction of the C domains with the plug (Supplementary Fig. 7). Only FimC-FimH chaperone-adhesin complexes are able to activate the FimD usher^{13,18,29}. Therefore, masking of the C domains would allow the usher to sample chaperone-subunit complexes in the periplasm via its N domain, with only FimC-FimH initiating pilus assembly by triggering release of the plug from the channel and freeing the C domains (Supplementary Fig. 7). Domain masking thus provides a mechanism to ensure assembly of a functional pilus fiber with the adhesin at its tip, poised to bind host cell receptors.

The plug domain is essential for the function of the usher in pilus biogenesis^{22,37,38}. The plug occupies the channel of the *apo* usher, and we show here that the plug also masks the C domains of the *apo* usher. However, these functions are related to maintenance of the usher in its inactive state. We found that the plug domain is not needed for recruitment of chaperone-subunit complexes to the usher or formation of stable pilus assembly intermediates *in vivo*. Instead, we found that the plug is required for efficient polymerization of the pilus fiber. The phenotype of the Δ plug mutant is similar to the phenotype obtained previously for mutations in the FimD N domain that affect the catalytic activity of the usher³⁹. The catalytic activity of the usher is postulated to be due to optimal positioning of chaperone-subunit complexes to promote the DSE reaction²³. The N domain is connected to the usher by a flexible linker and its location in the periplasm is dynamic. In the activated usher, the plug resides in the periplasm, adjacent to the N domain (Supplementary Fig. 1d)^{23,27}. We propose that the plug contributes to the catalytic activity of the usher by fixing orientation of the N domain relative to C domains. Thus, the location of the plug may act as a central switch that determines the activation state of the usher. In the resting usher, the plug closes the channel and masks the C domains. Expulsion

of the plug to the periplasm then activates the usher by (i) opening the channel, (ii) unmasking the C domains, and (iii) ensuring optimal positioning of the N domain to promote subunit-subunit interactions and catalyze fiber polymerization.

The usher monomer appears to be sufficient for pilus biogenesis, yet the usher forms dimeric and possibly higher order oligomers in the bacterial OM^{20,23,30-32}. A previous cryo-EM structure of a type 1 pilus assembly intermediate showed that only one usher molecule provides the channel for secretion of the pilus fiber, with the additional usher appearing idle²⁰. Thus, whether the usher oligomer makes a functional contribution to pilus biogenesis has been a subject of debate. We show here that co-expression of FimD_{ΔNΔplug} and FimD_{ΔC1ΔC2} ushers results in assembly of adhesive pili on the bacterial surface. Pilus biogenesis by these ushers necessitates that the N and C domains from different usher molecules cooperatively interact, providing a mechanistic basis for the function of the usher oligomer (Supplementary Fig. 7). Analysis of various combinations of FimD deletion mutants revealed that a plug domain is required for successful complementation, but the plug cannot be present on the same usher as the C domains. The requirement for the plug together with the N domain emphasizes the active role of the plug in the catalytic activity of the usher. The finding that complementation does not work when the plug is present together with the C domains reflects our finding that the plug masks the C domains in the inactive usher. This confirms the physiological relevance of domain masking to maintenance of the usher in the inactive state and to regulation of pilus biogenesis *in vivo*. In a prior study, we found that PapC C-terminal deletion mutants could interact with the FimD usher to drive assembly of P pili on the bacterial surface by the Fim system²⁸. This supports the formation of cooperative interactions between different ushers and the presence of a functional usher oligomer in bacteria. The FimH adhesin was also required for functional interaction between PapC and FimD in the prior study, suggesting that FimD needed to be activated by binding to the adhesin²⁸. In light of the results from the current study, we can now

understand that the C domains of FimD were masked and unavailable to participate in pilus assembly prior to usher activation.

Our experiments reveal mechanisms by which molecular machines such as the usher regulate and harness protein-protein interactions for biogenesis of complex organelles. The usher monomer is sufficient for pilus assembly and secretion, yet we demonstrate that the usher may function as an oligomer in bacteria. We propose that identical usher molecules act in an asymmetric manner during pilus biogenesis, with multiple ushers serving to recruit chaperone-subunit complexes to the OM, but only one usher providing the active translocation channel (Supplementary Fig. 7). Such an arrangement may enhance the catalytic activity of the usher by increasing the local concentration of chaperone-subunit complexes, and may allow for greater regulatory control of fiber polymerization through usher-usher interactions or changes in the oligomeric state of the usher. Other transporters found in both prokaryotes and eukaryotes also exist as oligomeric complexes⁴²⁻⁴⁵. Studies suggest that these complexes may also function in an asymmetric manner, with the oligomeric arrangement providing additional binding sites or allowing regulatory interactions^{42,45-47}. Thus, the use of identical channels in an asymmetric manner may be a common strategy employed by diverse transport systems.

ACKNOWLEDGEMENTS

We thank the Schultz laboratory (Scripps Research Institute) for providing plasmid pEVOL-pBpF. We thank Susan Van Horn of the Stony Brook University Central Microscopy Imaging Center and Vinaya Sampath (Stony Brook University) for assistance with electron microscopy. We thank John Haley, Dwight Martin and Robert Rieger of the Stony Brook Proteomics Center for performing the mass spectrometry analysis and for helpful discussions. We thank Suzanne Scarlata (Stony Brook University), Wali Karzai (Stony Brook University), Karen W. Dodson (Washington University), and Anne H. Delcour (University of Houston) for helpful discussions and critical reading of the manuscript.

This study was supported by National Institutes of Health (NIH) grants R01GM062987 (to D.G.T. and H.L.) and R01AI029549 (to S.J.H.). G.T.W. was supported by Medical Scientist Training Program award T32GM008444 and National Research Service Award F30AI112252 from the NIH. The Stony Brook Proteomics Center receives support from NIH award S10RR023680.

REFERENCES

1. Nuccio, S.P. & Baumber, A.J. Evolution of the chaperone/usher assembly pathway: fimbrial classification goes Greek. *Microbiol. Mol. Biol. Rev.* **71**, 551-575 (2007).
2. Zav'yalov, V., Zavialov, A., Zav'yalova, G. & Korpela, T. Adhesive organelles of Gram-negative pathogens assembled with the classical chaperone/usher machinery: structure and function from a clinical standpoint. *FEMS Microbiol. Rev.* **34**, 317-378 (2010).
3. Geibel, S. & Waksman, G. The molecular dissection of the chaperone-usher pathway. *Biochim. Biophys. Acta* **1843**, 1559-1567 (2014).
4. Thanassi, D.G., Bliska, J.B. & Christie, P.J. Surface organelles assembled by secretion systems of Gram-negative bacteria: diversity in structure and function. *FEMS Microbiol. Rev.* **36**, 1046-1082 (2012).
5. Mulvey, M.A. *et al.* Induction and evasion of host defenses by type 1-piliated uropathogenic *Escherichia coli*. *Science* **282**, 1494-1497 (1998).
6. Roberts, J.A. *et al.* The Gal(alpha1-4)Gal-specific tip adhesin of *Escherichia coli* P-fimbriae is needed for pyelonephritis to occur in the normal urinary tract. *Proc. Natl. Acad. Sci. USA* **91**, 11889-11893 (1994).
7. Jones, C.H. *et al.* FimH Adhesin of Type-1 Pili Is Assembled into a Fibrillar Tip Structure in the *Enterobacteriaceae*. *Proc. Natl. Acad. Sci. U S A* **92**, 2081-2085 (1995).
8. Hahn, E. *et al.* Exploring the 3D molecular architecture of *Escherichia coli* type 1 pili. *J. Mol. Biol.* **323**, 845-857 (2002).
9. Lycklama, A.N.J.A. & Driessen, A.J. The bacterial Sec-translocase: structure and mechanism. *Philos. Trans. R. Soc. Lond. B Biol. Sci.* **367**, 1016-1028 (2012).
10. Choudhury, D. *et al.* X-ray structure of the FimC-FimH chaperone-adhesin complex from uropathogenic *Escherichia coli*. *Science* **285**, 1061-1066 (1999).

11. Sauer, F.G. *et al.* Structural basis of chaperone function and pilus biogenesis. *Science* **285**, 1058-1061 (1999).
12. Zavialov, A.V. *et al.* Structure and biogenesis of the capsular F1 antigen from *Yersinia pestis*: preserved folding energy drives fiber formation. *Cell* **113**, 587-596 (2003).
13. Nishiyama, M., Ishikawa, T., Rechsteiner, H. & Glockshuber, R. Reconstitution of pilus assembly reveals a bacterial outer membrane catalyst. *Science* **320**, 376-379 (2008).
14. Sauer, F.G., Pinkner, J.S., Waksman, G. & Hultgren, S.J. Chaperone priming of pilus subunits facilitates a topological transition that drives fiber formation. *Cell* **111**, 543-551 (2002).
15. Rose, R.J. *et al.* Unraveling the molecular basis of subunit specificity in P pilus assembly by mass spectrometry. *Proc. Natl. Acad. Sci. U S A* **105**, 12873-12878 (2008).
16. Nishiyama, M. & Glockshuber, R. The outer membrane usher guarantees the formation of functional pili by selectively catalyzing donor-strand exchange between subunits that are adjacent in the mature pilus. *J. Mol. Biol.* **396**, 1-8 (2010).
17. Li, Q. *et al.* The differential affinity of the usher for chaperone-subunit complexes is required for assembly of complete pili. *Mol. Microbiol.* **76**, 159-172 (2010).
18. Saulino, E.T., Thanassi, D.G., Pinkner, J.S. & Hultgren, S.J. Ramifications of kinetic partitioning on usher-mediated pilus biogenesis. *EMBO J.* **17**, 2177-2185 (1998).
19. Volkan, E. *et al.* Domain activities of PapC usher reveal the mechanism of action of an *Escherichia coli* molecular machine. *Proc. Natl. Acad. Sci. U S A* **109**, 9563-9568 (2012).
20. Remaut, H. *et al.* Fiber formation across the bacterial outer membrane by the chaperone/usher pathway. *Cell* **133**, 640-652 (2008).
21. Nishiyama, M. *et al.* Structural basis of chaperone-subunit complex recognition by the type 1 pilus assembly platform FimD. *EMBO J.* **24**, 2075-2086 (2005).

22. Huang, Y., Smith, B.S., Chen, L.X., Baxter, R.H. & Deisenhofer, J. Insights into pilus assembly and secretion from the structure and functional characterization of usher PapC. *Proc. Natl. Acad. Sci. U S A* **106**, 7403-7407 (2009).
23. Phan, G. *et al.* Crystal structure of the FimD usher bound to its cognate FimC-FimH substrate. *Nature* **474**, 49-53 (2011).
24. Ng, T.W., Akman, L., Osisami, M. & Thanassi, D.G. The usher N terminus is the initial targeting site for chaperone-subunit complexes and participates in subsequent pilus biogenesis events. *J. Bacteriol.* **186**, 5321-5331 (2004).
25. Dubnovitsky, A.P. *et al.* Conserved hydrophobic clusters on the surface of the Caf1A usher C-terminal domain are important for F1 antigen assembly. *J. Mol. Biol.* **403**, 243-259 (2010).
26. Eidam, O., Dworkowski, F.S., Glockshuber, R., Grutter, M.G. & Capitani, G. Crystal structure of the ternary FimC-FimF(t)-FimD(N) complex indicates conserved pilus chaperone-subunit complex recognition by the usher FimD. *FEBS Lett.* **582**, 651-655 (2008).
27. Geibel, S., Procko, E., Hultgren, S.J., Baker, D. & Waksman, G. Structural and energetic basis of folded-protein transport by the FimD usher. *Nature* **496**, 243-246 (2013).
28. Shu Kin So, S. & Thanassi, D.G. Analysis of the requirements for pilus biogenesis at the outer membrane usher and the function of the usher C-terminus. *Mol. Microbiol.* **60**, 364-375 (2006).
29. Munera, D., Hultgren, S. & Fernandez, L.A. Recognition of the N-terminal lectin domain of FimH adhesin by the usher FimD is required for type 1 pilus biogenesis. *Mol. Microbiol.* **64**, 333-346 (2007).
30. Thanassi, D.G. *et al.* The PapC usher forms an oligomeric channel: implications for pilus biogenesis across the outer membrane. *Proc. Natl. Acad. Sci. U S A* **95**, 3146-3151 (1998).

31. Li, H. *et al.* The outer membrane usher forms a twin-pore secretion complex. *J. Mol. Biol.* **344**, 1397-1407 (2004).
32. Allen, W.J., Phan, G., Hultgren, S.J. & Waksman, G. Dissection of pilus tip assembly by the FimD usher monomer. *J. Mol. Biol.* **425**, 958-967 (2013).
33. Young, T.S., Ahmad, I., Yin, J.A. & Schultz, P.G. An enhanced system for unnatural amino acid mutagenesis in *E. coli*. *J. Mol. Biol.* **395**, 361-374 (2010).
34. Chin, J.W., Martin, A.B., King, D.S., Wang, L. & Schultz, P.G. Addition of a photocrosslinking amino acid to the genetic code of *Escherichia coli*. *Proc. Natl. Acad. Sci. U S A* **99**, 11020-11024 (2002).
35. Royer, C.A. & Scarlata, S.F. Fluorescence approaches to quantifying biomolecular interactions. *Methods Enzymol.* **450**, 79-106 (2008).
36. Morrissey, B. *et al.* The role of chaperone-subunit usher domain interactions in the mechanism of bacterial pilus biogenesis revealed by ESI-MS. *Mol. Cell. Proteomics* **11**, M111.015289 (2012).
37. Mappingire, O.S., Henderson, N.S., Duret, G., Thanassi, D.G. & Delcour, A.H. Modulating effects of the plug, helix and N- and C-terminal domains on channel properties of the PapC usher. *J. Biol. Chem.* **284**, 36324-36333 (2009).
38. Yu, X. *et al.* Caf1A usher possesses a Caf1 subunit-like domain that is crucial for Caf1 fibre secretion. *Biochem. J.* **418**, 541-551 (2009).
39. Henderson, N.S., Ng, T.W., Talukder, I. & Thanassi, D.G. Function of the usher N-terminus in catalysing pilus assembly. *Mol. Microbiol.* **79**, 954-967 (2011).
40. Thanassi, D.G., Stathopoulos, C., Karkal, A. & Li, H. Protein secretion in the absence of ATP: the autotransporter, two-partner secretion, and chaperone/usher pathways of Gram-negative bacteria. *Molec. Membr. Biol.* **22**, 63-72 (2005).

41. Nishiyama, M., Vetsch, M., Puorger, C., Jelesarov, I. & Glockshuber, R. Identification and characterization of the chaperone-subunit complex-binding domain from the type 1 pilus assembly platform FimD. *J. Mol. Biol.* **330**, 513-525 (2003).
42. Deville, K. *et al.* The oligomeric state and arrangement of the active bacterial translocon. *J. Biol. Chem.* **286**, 4659-4669 (2011).
43. Rehling, P. *et al.* Protein insertion into the mitochondrial inner membrane by a twin-pore translocase. *Science* **299**, 1747-1751 (2003).
44. Ahting, U. *et al.* Tom40, the pore-forming component of the protein-conducting TOM channel in the outer membrane of mitochondria. *J. Cell Biol.* **153**, 1151-1160 (2001).
45. Reichow, S.L. *et al.* Allosteric mechanism of water-channel gating by Ca²⁺-calmodulin. *Nat. Struct. Mol. Biol.* **20**, 1085-1092 (2013).
46. Dalal, K., Chan, C.S., Sligar, S.G. & Duong, F. Two copies of the SecY channel and acidic lipids are necessary to activate the SecA translocation ATPase. *Proc. Natl. Acad. Sci. U S A* **109**, 4104-4109 (2012).
47. Mao, C. *et al.* Stoichiometry of SecYEG in the active translocase of *Escherichia coli* varies with precursor species. *Proc. Natl. Acad. Sci. U S A* **110**, 11815-11820 (2013).

METHODS

Strains and plasmids. The bacterial strains and plasmids used in this study are listed in Supplementary Table 2. Unless otherwise noted, bacteria were grown at 37°C with aeration in LB medium. When appropriate, the growth medium was supplemented with antibiotics as follows: 100 µg/ml ampicillin (Amp); 50 µg/ml kanamycin (Kan); 100 µg/ml spectinomycin (Spec); 25 µg/ml chloramphenicol (CIm); 15 µg/ml tetracycline (Tet).

The molecular biology techniques and primers used to construct the plasmids made in this study are listed in Supplementary Table 3. *E. coli* DH5α was used as the host strain for plasmid manipulations. The FimD *amber* mutants used for site-directed photocrosslinking were derived from plasmids pNH213 or pNH400 using QuikChange Site-Directed Mutagenesis (Stratagene). Plasmid pNH213 encodes the FimD usher with a C-terminal, thrombin-cleavable, polyhistadine tag (His-tag) under isopropyl-β-D-thiogalactoside (IPTG)-inducible expression. For pNH400, the His-tag of plasmid pNH213 was switched to a Step-tag using site-directed, ligase-independent mutagenesis (SLIM)^{48,49}. The FimC cysteine mutants for fluorescence labeling were derived from pETS1000 using QuikChange mutagenesis. Plasmid pETS1000 encodes the FimC chaperone with a C-terminal His-tag under arabinose-inducible expression. Plasmid pNH324, encoding FimD_{Δplug}, was derived from pNH213 using SLIM to delete residues 244-323. In addition to deletion of the plug domain, an N243G substitution mutation was created. Similarly, the plug domain was deleted from plasmids pNH295 and pNH296, encoding FimD_{ΔC1ΔC2} and FimD_{ΔN}, respectively, to make plasmids pNH423 and pGW117. All constructs generated using SLIM or QuikChange mutagenesis methods were sequenced to verify that the correct mutations were made.

In vivo site-directed photocrosslinking. Strain SF100 was transformed with plasmid pEVOL-pBpF, encoding an arabinose-inducible *amber* suppressor tRNA and aminoacyl-tRNA synthetase, allowing incorporation of *pBpa* at *amber* stop codons (TAG)³³. Strain SF100/pEVOL-pBpF was then transformed with plasmid pNH212, encoding IPTG-inducible FimC and FimH proteins. Finally, strain SF100/pEVOL-pBpF + pNH212 was transformed with plasmids for IPTG-inducible expression of His-tagged wild-type (WT) FimD (pNH213) or FimD F4 (pNH319), Y704 (pNH320), T717 (pNH321), or Y788 (pNH329) *amber* codon mutants. Overnight cultures were diluted 1:20 into 30–50 ml fresh LB containing 0.2 mM *pBpa* (VWR). Cultures were induced at OD₆₀₀ = 0.6 with 0.1% arabinose and 50 μM IPTG for 1–2 h. Cultures were pelleted and resuspended in 1 ml 20 mM Tris-HCl (pH 8.0), transferred to wells in an untreated six-well culture plate (CytoOne), and exposed to a UV lamp (365 nm, 100 W, Fisher Scientific) for 10 min. Exposed bacteria were then transferred to microcentrifuge tubes and pelleted at maximum speed in a microcentrifuge for 15 min at 4 °C. Pellets were weighed and resuspended in 500 μl BugBuster Master Mix (Novagen) per 0.1 g wet weight. EDTA-free Complete protease inhibitor (Roche) was added, and the samples were rocked for 20 min at room temperature. Samples were then spun at maximum speed in a microcentrifuge for 20 min at 4 °C, and supernatant fractions were transferred to clean tubes. Imidazole was added to 20 mM, 50 μl of 50% Ni-NTA agarose beads (Qiagen) were added, and samples were rocked for 30 min at room temperature. The beads were washed 3 times with 1 ml 20 mM Tris-HCl (pH 8.0), 0.3 M NaCl, 20 mM imidazole, and then boiled in 60 μl of 2X SDS-PAGE sample buffer. Boiled samples were separated by SDS-PAGE, and analyzed either by staining with Coomassie blue or immunoblotting with anti-His-tag (Covance), anti-FimC-FimH, or anti-FimC-FimG antibodies. The blots were developed with alkaline phosphatase-conjugated secondary antibodies and BCIP (5-bromo-4-chloro-3-indolylphosphate)-NBT (nitroblue tetrazolium) substrate (KPL).

For some experiments, SF100/pEVOL-pBpF + pNH212 strains expressing Strep-tagged instead of His-tagged FimD were used (plasmids pNH400 through pNH404). For these experiments, following UV exposure, OM fractions were isolated as described²⁴. The OM fractions were separated by SDS-PAGE and analyzed by immunoblotting with anti-His-tag or anti-FimC-FimH antibodies, as above. The expression and folding of the FimD *amber* mutants in the OM was compared with WT FimD, as described below. SF100/pEVOL-pBpF was used as the host strain for these experiments and the bacteria were grown in the presence of 0.2 mM pBpa. The ability of the FimD *amber* mutants to assemble adhesive pili on the bacterial surface was compared with WT FimD using the HA assay, as described below. For these assays, MM294 Δ *fimD*/pEVOL-pBpF was used as the host strain and the bacteria were grown in the presence of 0.2 mM pBpa.

Mass spectrometry analysis of crosslinked products. Excised gel pieces were destained, reduced, alkylated and digested with trypsin (Promega Gold, Mass Spectrometry Grade), essentially as described⁵⁰. The resulting concentrated peptide extract was diluted into a solution of 2% Acetonitrile (ACN), 0.1% Formic Acid (FA) (buffer A) for analysis. The peptide mixture was analyzed by automated microcapillary liquid chromatography-tandem mass spectrometry. Fused-silica capillaries (100 μ m i.d.) were pulled using a P-2000 CO₂ laser puller (Sutter Instruments) to a < 5 mm i.d. tip, and packed with 10 cm of 5 μ m ProntoSil 120-5-C18H material (Agilent) using a pressure bomb. The column was installed in-line with an Eksigent Nano2D High Performance Liquid Chromatography (HPLC) pump running at 300 nl min⁻¹. The column was equilibrated in buffer A, and the peptide mixture was loaded onto the column using an autosampler. The HPLC separation was provided by a gradient between buffer A and buffer B (98% ACN, 0.1% FA). The HPLC gradient was held constant at 100% buffer A for 10 min after peptide loading, followed by a 35-min gradient from 0% buffer B (100% Buffer A) to 40% buffer B. Then, another gradient was performed for 3 min to 80% buffer B, where it was held

constant for 2 min. Finally, the gradient was changed from 80% buffer B to 100% buffer A over 1 min, and then held constant at 100% buffer A for 29 more minutes. The application of a 1.8 kV distal voltage electrosprayed the eluted peptides directly into a Thermo Fisher Scientific LTQ XL ion trap mass spectrometer equipped with a custom built nanoLC electrospray ionization source. Full mass spectra (MS) were recorded on the peptides over a 400-2000 m/z range, followed by five tandem mass (MS/MS) events sequentially generated in a data-dependent manner on the first, second, third, fourth and fifth most intense ions selected from the full MS spectrum (at 35% collision energy). Mass spectrometer scan functions and HPLC solvent gradients were controlled by the Xcalibur data system (ThermoFinnigan, San Jose, CA). The resultant MS/MS spectra were extracted from the RAW file with Readw.exe (<http://sourceforge.net/projects/sashimi>). The resulting mzXML file contains all the data for all MS/MS spectra and can be read by the subsequent analysis software. The MS/MS data were searched using InsPecT⁵¹ and GPM XITandem against the Ecoli_K12 UniProt database (downloaded 3/19/2013) with optional modifications: +16 on Methionine, +57 on Cysteine, and +80 on Threonine, Serine and Tyrosine. Only peptides with a P value of ≤ 0.01 were analyzed further. Common contaminants (e.g. keratins) were removed from the database. Proteins identified by at least 2 distinct peptides within a sample were considered valid.

Purification of FimD and FimC-FimH for affinity measurements. The WT FimD usher and FimD domain deletion mutants contained C-terminal, thrombin-cleavable His-tags and were purified as described⁵². Briefly, 6 l cultures of strain Tuner harboring plasmid pNH213 (WT FimD), pNH295 (FimD $_{\Delta C1\Delta C2}$), pNH317 (FimD $_{\Delta C2}$), pNH296 (FimD $_{\Delta N}$), pNH324 (FimD $_{\Delta plug}$), or pGW117 (FimD $_{\Delta N\Delta plug}$) were induced for usher expression at $OD_{600} = 0.6$ with 100 μ M IPTG and grown overnight at room temperature. Bacteria were lysed using a French press and the OM fraction was isolated by Sarkosyl extraction and centrifugation. OM fractions were then solubilized in 20 mM Tris-HCl (pH 8), 0.3 M NaCl, 1% dodecyl-maltopyranoside (DDM;

Anatrace). Imidazole was added to 20 mM and the samples were loaded onto a cobalt affinity column using an FPLC apparatus (GE Healthcare). The bound FimD protein was eluted using an imidazole step gradient in buffer 20 mM Tris-HCl (pH 8), 0.3 M NaCl, 10 mM lauryl(dimethyl)amine oxide (LDAO; Anatrace). The His-tag was cleaved by digestion with thrombin overnight, and then the sample was passed again over a cobalt affinity column coupled to a benzamidine column (GE Healthcare). The pure, His-tag-free FimD was collected in the flow-through fraction. The purified protein was dialyzed into 20 mM HEPES (pH 7.5), 150 mM NaCl, 5 mM LDAO, and concentrated using a Millipore Ultrafree centrifugal concentrator (50 kDa molecular weight cutoff). Protein concentrations were determined using the bicinchoninic acid (BCA) protein assay (Pierce).

FimC-FimH complexes were purified from strain Tuner/pHJ20 harboring plasmid pGW1 (FimC_{T51C}), pGW2 (FimC_{N86C}), or pGW3 (FimC_{Q19C}). Plasmid pHJ20 encodes IPTG-inducible FimH, and plasmids pGW1–3 encode arabinose-inducible, His-tagged FimC with the indicated cysteine substitutions. Purification was performed as described⁵². Briefly, 2 l cultures were grown at 37 °C and induced at OD₆₀₀ = 0.6 with 0.002% arabinose and 1 mM IPTG for 2 h. Periplasm fractions were isolated by EDTA-lysozyme treatment and dialyzed into 20 mM Tris-HCl (8.0), 0.3 M NaCl. Imidazole was added to 20 mM and samples were loaded onto a nickel affinity column using an FPLC apparatus. Bound FimC-FimH complex was eluted using an imidazole step gradient. Fractions containing FimC-FimH were pooled and dialyzed into 20 mM MES (pH 5.4). The samples were then run on a Resource S column (GE Healthcare) and eluted using a linear NaCl gradient, to separate excess unbound FimC chaperone from FimC-FimH chaperone-adhesin complex.

Fluorescence-based affinity assay. Fluorescence labeling reactions and titration experiments were performed as described^{17,35}. FimC_{Q19C}, FimC_{T51C}, or FimC_{N86C}-FimH complexes (500 nM)

were labeled with the thiol-reactive probe coumarin maleimide (Life Technologies) for 2 h at 4 °C at a 5:1 probe:protein molar ratio. For labeling, the pH of the protein solution was first raised to 8.0 via the addition of K_2HPO_4 . Unbound probe was removed via dialysis against 20 mM HEPES (pH 7.5), 150 mM NaCl, and 5 mM LDAO was added to the final exchanged solution. Labeling efficiency was calculated using Beer's Law, and was typically > 80%.

Fluorescence measurements were performed using a PC1 photon-counting spectrofluorometer (ISS), as described¹⁷. Coumarin-labeled chaperone-subunit complexes were diluted to 25 nM and 120 μ l was transferred to a 3 mm microcuvette. Purified FimD was then titrated into the FimC-FimH solution. The fluorophore was excited at 384 nm, and its emission spectrum was measured from 420-520 nm with a step size of 2 nm. Variability in lamp intensity was accounted for using Vinci (ISS) data acquisition software. The integral of the curve was calculated, providing the total emission intensity. Buffer measurements were also performed, and background emissions were subtracted. Data were normalized to account for dilution during titration, and set to a scale of 0 (starting value) to 1 (the final value). Apparent equilibrium bimolecular dissociation constants (K_d) were obtained by fitting the data using a sigmoidal curve function in Prism (GraphPad) and solving for the inflection point. Each titration curve shown is the result of at least three independent experiments with three replicates per experiment. All of our observed K_d 's were independent of starting FimC-FimH concentrations (below the dissociation constant), and thus were dependent only on the mass action of the titrant, FimD. Statistical comparison of K_d 's for FimD mutants with WT FimD was performed using a two-tailed t test in Prism (GraphPad). Comparison of the different FimC cysteine substitution mutants was performed using one-way analysis of variance and Tukey's multiple-comparison post test. P values < 0.05 were considered significant.

Analysis of usher expression and folding in the OM. The expression levels and folding of the FimD mutants in the OM were compared to WT FimD, as described³⁹. Briefly, OM fractions were isolated by French press disruption and Sarkosyl extraction, and proper folding of the ushers was determined by heat-modifiable mobility on SDS-PAGE. Strain SF100 was used as the host strain for these studies.

Hemagglutination (HA) assay. HA assays were performed by serial dilution in microtiter plates, as described³⁹. HA titers were determined visually and are reported as the greatest fold dilution of bacteria able to agglutinate guinea pig red blood cells (Colorado Serum Company). For each HA assay, at least three independent experiments were performed, with three replicates per experiment. Analysis of the FimC WT and cysteine substitution mutants was performed in strain MM294 Δ *fimC*, which contains a *fimC* deletion in the chromosomal *fim* operon. Analysis of the FimD WT and mutant ushers was performed in strain MM294 Δ *fimD*, which contains a *fimD* deletion in the chromosomal *fim* operon. The experiments in which FimD WT or domain deletion mutant ushers were co-expressed were also done in strain MM294 Δ *fimD*. Bacteria harboring appropriate FimD or FimC plasmids were grown statically for 24–48 h to induce the chromosomal *fim* genes, and then FimD or FimC expression was induced with 50 μ M IPTG or 0.15% arabinose, respectively, for an additional 3 h with shaking at 100 rpm. To test the role of OmpA in type 1 pilus biogenesis, HA titers were determined for strain JF568 and its isogenic *ompA*⁻ derivative JF699. The strains were grown statically for 24–48 h to induce the chromosomal *fim* genes. For analysis of assembly of FimG-FimH type 1 pilus tips, strain AAEC185/pNH222 (encoding FimC, FimG, and FimH) was transformed with the FimD expression plasmids pNH213 (WT FimD) or pNH324 (FimD Δ _{plug}). HA titers were determined from strains grown with aeration and induced at OD₆₀₀ = 0.6 with 50 μ M IPTG and 0.1% arabinose for 1 h.

Electron microscopy (EM). Whole bacteria, negative-stain transmission EM was performed as described²⁴. Aliquots (1 ml) of cultures grown for the HA assay were washed with PBS and resuspended in 1.5 ml PBS. Bacteria were fixed with 1% glutaraldehyde in PBS, washed with PBS followed by water, and then stained for 20 s with phosphotungstic acid. Grids were examined on a TECNAI 12 BioTwin G02 microscope (FEI) and representative images were acquired with an XR-60 CCD digital camera system (Advanced Microscopy Techniques).

Co-purification of type 1 pilus assembly intermediates with WT and Δ plug FimD ushers.

Co-purification assays were performed as previously described³⁹. Briefly, OM fractions were isolated by French press disruption and Sarkosyl extraction from strain AAEC185/pNH222 harboring plasmids pNH213 or pNH324, grown as described for the HA assay. OM fractions were solubilized with the non-denaturing detergent DDM, and the His-tagged FimD was purified by cobalt affinity chromatography. FimD-containing fractions from the column were incubated for 10 min at 25 or 95°C in SDS-PAGE sample buffer, separated by SDS-PAGE, and immunoblotted with anti-FimC-FimH or anti-FimC-FimG antibodies to detect pilus assembly intermediates that co-purified with the usher. Immunoblots were developed with alkaline phosphatase-conjugated secondary antibodies and BCIP-NBT substrate.

METHODS REFERENCES

48. Chiu, J., March, P.E., Lee, R. & Tillett, D. Site-directed, Ligase-Independent Mutagenesis (SLIM): a single-tube methodology approaching 100% efficiency in 4 h. *Nucleic Acids Res.* **32**, e174 (2004).
49. Chiu, J., Tillett, D., Dawes, I.W. & March, P.E. Site-directed, Ligase-Independent Mutagenesis (SLIM) for highly efficient mutagenesis of plasmids greater than 8kb. *J. Microbiol. Methods* **73**, 195-198 (2008).
50. Shevchenko, A., Wilm, M., Vorm, O. & Mann, M. Mass spectrometric sequencing of proteins silver-stained polyacrylamide gels. *Anal. Chem.* **68**, 850-858 (1996).
51. Tanner, S. *et al.* InsPecT: identification of posttranslationally modified peptides from tandem mass spectra. *Anal. Chem.* **77**, 4626-4639 (2005).
52. Henderson, N.S. & Thanassi, D.G. Purification of the outer membrane usher protein and periplasmic chaperone-subunit complexes from the P and type 1 pilus systems. *Methods Mol. Biol.* **966**, 37-52 (2013).

FIGURE LEGENDS

Figure 1, Werneburg *et al.*

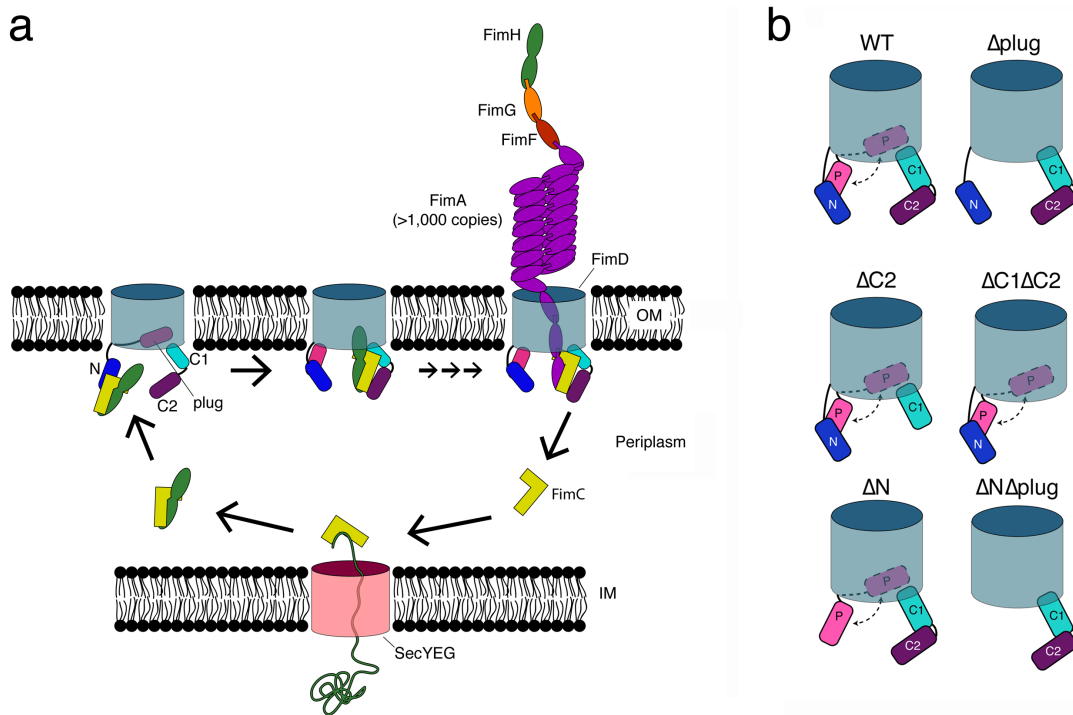


Figure 1. Models for type 1 pilus biogenesis and usher domain architecture. (a) Assembly of type 1 pili by the CU pathway. Pilus subunits traverse the inner membrane (IM) via the Sec translocon. Upon entering the periplasm, the subunits form binary complexes with the FimC chaperone (yellow). The chaperone enables proper folding of pilus subunits via the DSC mechanism (see also Supplementary Fig. 1a). Chaperone-subunit complexes next interact with the FimD usher. The usher is depicted as a monomer, with its β -barrel channel domain in the OM and its N, plug, C1, and C2 domains indicated. Binding of a chaperone-adhesin complex (FimC-FimH) to the N domain activates the usher for pilus biogenesis. The plug is expelled from the usher channel to accommodate the FimH adhesin, and the FimC-FimH complex is handed off from the N to the C domains. The N domain is now free to recruit additional chaperone-subunit complexes, which undergo DSE with the last-incorporated subunit bound at the C domains (see also Supplementary Fig. 1b). Repeated rounds of subunit recruitment and DSE result in assembly of the pilus fiber in a top-down manner and secretion through the usher channel to the bacterial surface. **(b)** Cartoon representations of WT FimD and the domain-deletion mutants used in this study. The N, plug (P), C1, and C2 domains are indicated.

Figure 2, Werneburg *et al.*

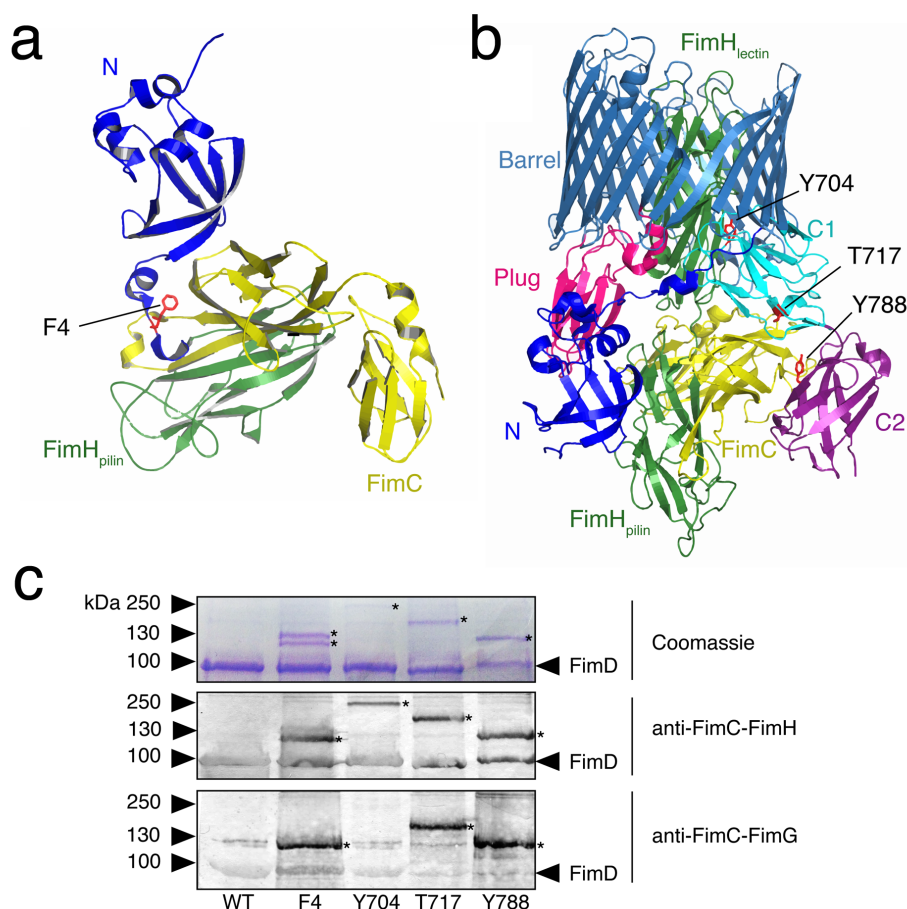


Figure 2. *In vivo* detection of FimC-FimH binding to the FimD usher. (a) Structure of the FimD N domain (blue) bound to a FimC-FimH pilin domain complex (yellow and green, respectively) (PDB ID: 1ZE3). FimD residue F4 is depicted in red in stick representation. F4 is in close proximity to the FimC chaperone (see also Supplementary Fig. 2a). (b) Structure of the FimD-FimC-FimH complex (PDB ID: 3RFZ). FimH is in green, FimC is in yellow, and the FimD domains are colored as in Figure 1. Residues Y704 (C1), T717 (C1), and Y788 (C2) are depicted in red in stick representation. Y704 is in close proximity to the FimH adhesin domain, whereas T717 and Y788 are in proximity to the chaperone (see also Supplementary Fig. 2b). (c) *In vivo*, site-directed photocrosslinking. His-tagged WT FimD or FimD F4 (N domain), Y704 (C1 domain), T717 (C1 domain), or Y788 (C2 domain) *amber* mutants were expressed together with FimC and FimH in *E. coli* strain SF100/pEVOL-pBpF. The bacteria were grown in the presence of *pBpa* and exposed to UV light to induce crosslinks. The purified His-tagged ushers and associated crosslinked products were analyzed by staining with Coomassie blue (top panel) or by immunoblotting with anti-FimC-FimH (middle panel) or anti-FimC-FimG (bottom panel) antibodies. Note that the anti-FimC-FimH antibody cross-reacts with the His-tag on FimD. See Supplementary Figure 3 for additional controls. The position of the FimD monomer is indicated on the right for each panel. The asterisks (*) mark FimD crosslinked products.

Figure 3, Werneburg *et al.*

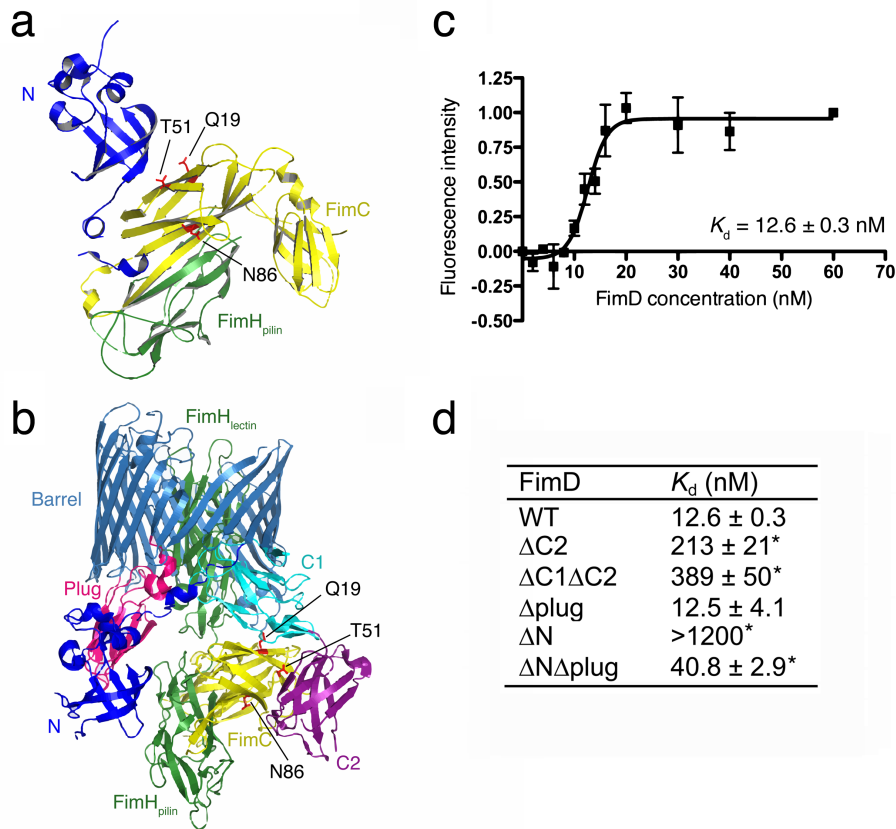


Figure 3. Binding affinities of FimC-FimH chaperone-adhesin complexes for WT and domain-deleted FimD ushers. Structures of the FimD N domain bound to a FimC-FimH pilin domain complex (a), and the FimD-FimC-FimH complex (b). The structures and colors are as in Figure 2. The FimC cysteine substitution sites Q19, T51, and N86 are shown in red in stick representation. These sites are in close proximity to the usher when FimC-FimH is bound at either the N or C domains (see also Supplementary Fig. 4). (c) Affinity of FimC-FimH for WT FimD. FimC-FimH was fluorescently labeled at FimC position Q19C with coumarin maleimide. Labeled FimC-FimH was added to cuvettes at 25 nM final concentration and fluorescence spectra were recorded as WT FimD was titrated into the cuvettes. The graph represents normalized changes in total fluorescence emission intensity plotted as a function of FimD concentration, where the total change in intensity was 20%. The data points represent means \pm SEM of three independent experiments, with three replicates per experiment. The K_d value was obtained by fitting the data to a sigmoidal curve. See also Supplementary Figure 5. (d) Affinities of FimC-FimH for FimD WT and domain deletion mutants. Affinities were calculated as in c. See also Supplementary Figure 6. *, $P < 0.005$ compared to WT FimD.

Figure 4, Werneburg *et al.*

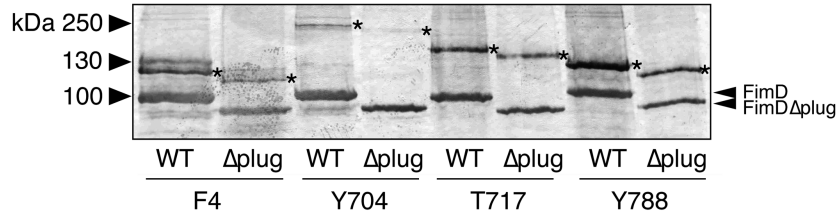


Figure 4. FimC-FimH binds to the N, C1, and C2 domains of the FimD_{Δplug} usher *in vivo*. His-tagged WT or Δplug FimD ushers containing *amber* mutations at positions F4 (N domain), Y704 (C1 domain), T717 (C1 domain), or Y788 (C2 domain) were expressed together with FimC and FimH in *E. coli* strain SF100/pEVOL-pBpF. The bacteria were grown in the presence of pBpa and exposed to UV light to induce crosslinks. The purified His-tagged ushers and associated crosslinked products were analyzed by immunoblotting with anti-FimC-FimH antibodies. Note that the anti-FimC-FimH antibody cross-reacts with the His-tag on FimD. The positions of the WT and Δplug FimD monomers are indicated on the right, and the asterisks (*) mark the crosslinked products. Note that the level of FimD_{Δplug} in the OM is lower than for WT FimD, explaining the weaker appearance of the crosslinked bands for the Δplug mutant.

Figure 5, Werneburg *et al.*

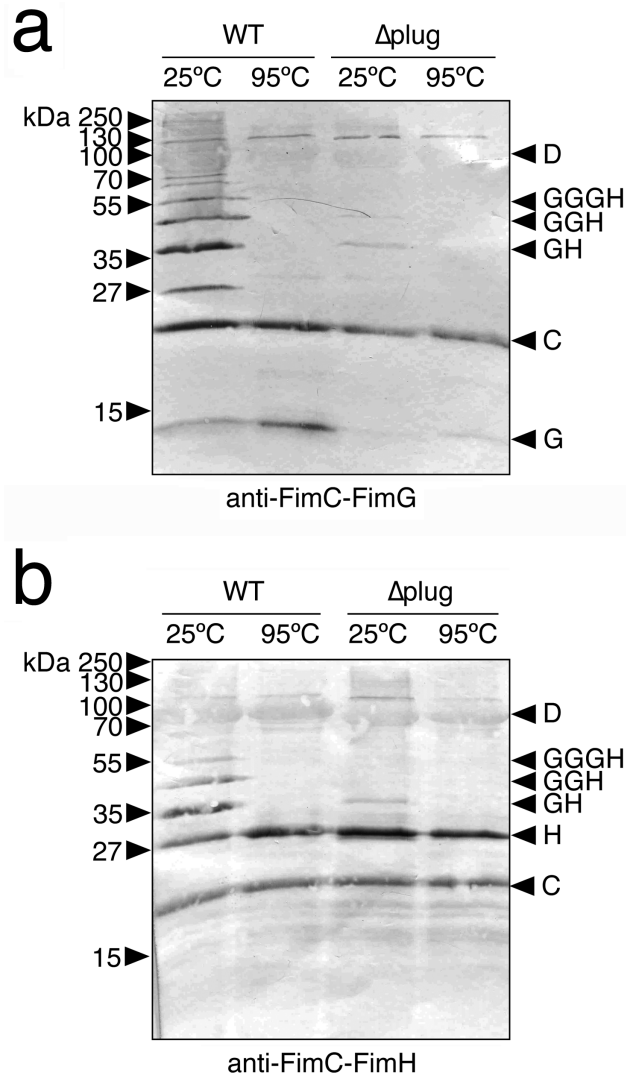


Figure 5. Assembly of type 1 pilus tip fibers by the WT and Δ plug FimD ushers. OM fractions were isolated from *E. coli* strain AAEC185 expressing FimC chaperone, FimG and FimH tip subunits, and His-tagged WT or Δ plug FimD usher. The His-tagged usher and associated pilus assembly intermediates were purified from the OM fractions by cobalt affinity chromatography. The purified samples were incubated at 25 or 95°C in sample buffer, subjected to SDS-PAGE, and immunoblotted with anti-FimC-FimG (**a**) or anti-FimC-FimH (**b**) antibodies. The identities of the pilus proteins and assembly intermediates are indicated on the right using single letters (C, FimC; G, FimG; H, FimH; D, FimD).

Figure 6, Werneburg *et al.*

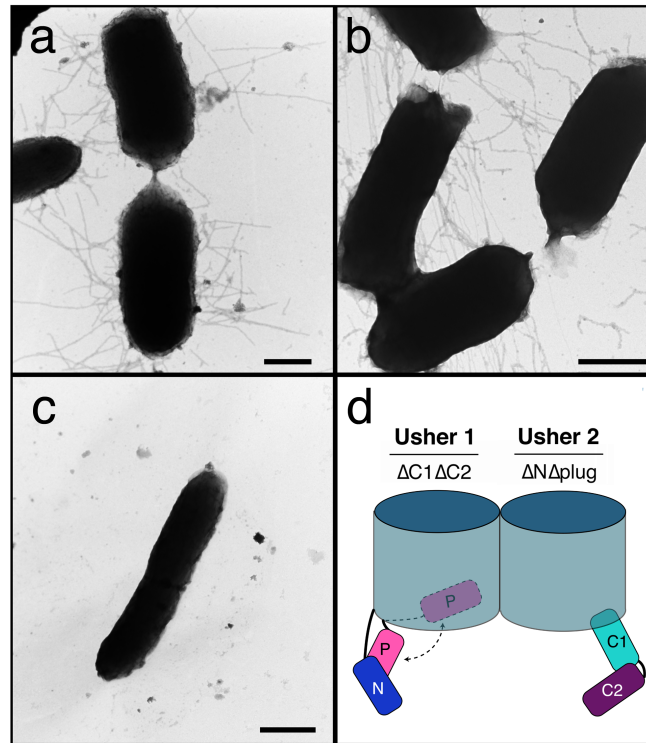


Figure 6. Co-expression of $FimD_{\Delta N\Delta plug}$ and $FimD_{\Delta C1\Delta C2}$ ushers results in pilus assembly on the bacterial surface. *E. coli* strain MM294 $\Delta fimD$ expressing WT FimD (a), $FimD_{\Delta N\Delta plug}$ together with $FimD_{\Delta C1\Delta C2}$ (b), or vector only (c) were examined by whole-bacteria, negative-stain transmission EM. The FimD expression plasmids used were as listed in Table 1. Scale bars = 500 nm. (d) Cartoon representations of the $FimD_{\Delta C1\Delta C2}$ (usher 1) and $FimD_{\Delta N\Delta plug}$ (usher 2) deletion mutants co-expressed in b. The N, plug (P), C1, and C2 domains present in each usher construct are indicated.

Table 1. Assembly of adhesive pili on the bacterial surface by co-expression of WT or domain-deleted FimD ushers

FimD	Plasmids	HA titer ^a
WT + WT	pNH382 + pNH213	128
$\Delta N + \Delta C1\Delta C2$	pNH383 + pNH295	0
$\Delta N\Delta\text{plug} + \Delta C1\Delta C2$	pGW217 + pNH295	32
$\Delta N\Delta\text{plug} + \text{vector}$	pGW217 + pMMB66	0
vector + $\Delta C1\Delta C2$	pTRYC + pNH295	0
$\Delta N + \Delta\text{plug}\Delta C1\Delta C2$	pNH383 + pNH423	0
$\Delta N\Delta\text{plug} + \Delta\text{plug}\Delta C1\Delta C2$	pGW217 + pNH423	0

^aHemagglutination (HA) titer is the maximum fold dilution of bacteria (strain MM294 ΔfimD expressing the indicated FimD constructs) able to agglutinate guinea pig red blood cells.